ELSEVIER

Solid State Sciences 4 (2002) 317–322

Solid State Sciences

www.elsevier.com/locate/ssscie

Phase relations, transparency and conductivity in Ga_2O_3–SnO_2–ZnO

G.B. Palmer [1], K.R. Poeppelmeier *

Department of Chemistry and Materials Research Center, Northwestern University, 2145 Sheridan road, Evanston, IL 60208-3113, USA

Dedicated to Martha Greenblatt on her 60th birthday

Abstract

Subsolidus phase relationships in the Ga_2O_3–SnO_2–ZnO system were determined at 1250 °C using solid state synthesis and X-ray powder diffraction. The two spinels, Zn_2SnO_4 and $ZnGa_2O_4$, formed a complete solid solution. The optical band gap of the spinel varied with composition from 3.6 eV (Zn_2SnO_4) to 4.7 eV ($ZnGa_2O_4$). All samples were white and insulating except those containing Ga-doped ZnO. The phase relations and physical properties of Ga_2O_3–SnO_2–ZnO were compared with those of In_2O_3–SnO_2–ZnO.

1. Introduction

Our study of the Ga_2O_3–SnO_2–ZnO system was motivated by a desire to understand the structure-to-property relations of transparent conducting oxides (TCOs). Because of their combination of visual light transparency and high electrical conductivity, TCOs (transparent conducting oxides) are regularly used as electrodes in solar cells, flat panel displays and other commercial devices. For instance, the industry TCO of choice, ITO (tin-doped indium oxide) has a typical conductivity of $1–5 \times 10^3$ S cm^{-1} and a transparency of 85–90% in thin films [1,2]. Although TCO applications are usually in film form, study of bulk phase relations and physical property trends can be useful for understanding fundamental materials properties. Previous study of the transparency, conductivity and phase relationships in the Ga_2O_3–In_2O_3–SnO_2 [3], Ga_2O_3–In_2O_3–ZnO [4], and In_2O_3–SnO_2–ZnO [5] systems resulted in the discovery of new TCO compounds and solid solutions [6].

Both SnO_2 and ZnO are good TCOs with conductivities comparable to ITO when properly doped [7,8]. Ga_2O_3 is not readily doped and thus has too low of a conductivity for direct use as a TCO. However, Ga^{3+} is present as a structural cation in several new multi-cation TCOs [9–11]. In addition, Ga^{3+} is a good dopant for ZnO-based TCO films [8]. Zn_2SnO_4 [12] and $ZnGa_2O_4$ [13] have been reported as TCO films. However, the conductivities of Zn_2SnO_4 and $ZnGa_2O_4$ were two and four orders of magnitude less, respectively, than ITO's conductivity.

2. Experimental

Synthesis. The starting materials were 99.99% Ga_2O_3, and 99.9% SnO_2 (cation basis, Aldrich Chemical Company, USA) and 99.99% ZnO (cation basis, Alfa Aeser Chemical Company, USA). Vendor supplied ICP analyses of the starting materials showed the following major impurities: 45 ppm Sn, 13 ppm Cu, and 11 ppm Al in Ga_2O_3; 50 ppm Fe, 50 ppm Sb, 30 ppm Bi, 20 ppm Pb, 10 ppm In, and 10 ppm Ca in SnO_2; and 20 ppm Pb, 10 ppm Na and 10 ppm Ca in ZnO. Prior to sample preparation, the starting material powders were calcined at high temperature in air to ensure the anionic content was all oxygen. Calcining produced negligible mass change. After calcining, the starting material powders were stored in a vacuum desiccator prior to sample preparation.

Table 1 shows the sample compositions. 2 g samples were ground together under acetone with an agate mortar and pestle. 1.27 cm (0.5 inch) pellets were uniaxially pressed in a steel die at 51.7 MPa (Carver 3392 Laboratory Press, USA). Sample pellets were fired in alumina crucibles. The pellets were buried in their constituent powders to minimize reaction with the alumina crucibles or evaporation of the metal oxides. Samples were initially heated at 1100 °C for approximately 4 days. The samples were then removed, reground and repelletized, prior to a 1250 °C heating of approximately 4 days. The furnace used for the final high tem-

* Correspondence and reprints.
E-mail address: krp@northwestern.edu (K.R. Poeppelmeier).
[1] Present address: McKinsey & Company Inc., Suite 4600, Georgia-Pacific Center, 133 Peachtree Street, Atlanta, GA 30303, USA.

1293-2558/02/$ – see front matter
PII: S1293-2558(01)01258-4

Table 1
Ga_2O_3–SnO_2–ZnO sample compositions and phase analysis

$GaO_{1.5}$ (%)	SnO_2 (%)	ZnO (%)	Phases observed[a]
15	25.83	59.17	spinel
30	18.33	51.67	spinel
45	10.83	44.17	spinel
10	15	75	spinel, U
45	35	20	spinel, rutile SnO_2
66.67	0	33.83	spinel
80	0	20	spinel, β-Ga_2O_3
90	5	5	spinel, β-Ga_2O_3, rutile SnO_2
75	12.5	12.5	spinel, β-Ga_2O_3, rutile SnO_2
30	45	45	spinel, rutile SnO_2
55	6	39	spinel
35	16	49	spinel
20	23.33	56.67	spinel
0	33.33	66.67	spinel
66.67	0	33.33	spinel
20	23.33	56.67	spinel
40	13.33	46.67	spinel
95	5	0	β-Ga_2O_3, rutile SnO_2
50	50	0	β-Ga_2O_3, rutile SnO_2
5	95	0	β-Ga_2O_3, rutile SnO_2
95	2.5	2.5	β-Ga_2O_3
20	10	70	spinel, U
50	0	50	spinel, U
2	0	98	U
30	5	65	spinel, U
100	0	0	β-Ga_2O_3
0	100	0	ZnO
0	95	5	spinel, ZnO
0	80	20	spinel, ZnO
0	66.67	33.33	spinel
0	33.33	66.67	spinel, rutile SnO_2
0	10	90	spinel, rutile SnO_2
0	5	95	rutile SnO_2
0	2	98	rutile SnO_2
0	0	100	rutile SnO_2

[a] U = unassigned peaks corresponding to distorted ZnO, layered Zn/Ga oxide compound(s), and/or ZnO. See text for further explanation.

perature heating had two independent thermocouples, which agreed within 10 °C. Samples were quenched from 1250 °C by removing the crucibles from the at-temperature furnace and allowing them to cool in lab air. Sample mass losses as a result of firing were less than 1%. Selected samples were reduced in flowing forming gas (7% H_2 / 93% N_2) for 10 hours at 500 °C.

X-ray crystallography. Powder X-ray diffraction was used to determine phase composition after both firings (Rigaku, USA). Copper K_α radiation was used at 40 kV and 20 mA. LiF (JCPDS Card No. 4-857, Copper K_{α_1}) was used as an internal X-ray standard. The average shift of the observed LiF peaks was used to make an off-axis correction (2θ shift) to the sample peaks. The X-ray peaks were fitted using XRAYFIT [14]. Lattice parameters were calculated with a least squares averaging program, POLSQ [15], using the weighted-average K_α wavelength, 1.5418 Å. The precision of resulting lattice parameters was about 0.005 Å (for spinel).

Electronic measurements. Room temperature electrical conductivities of as-fired pellets were measured with a spring-loaded linear four probe apparatus. Excitation currents ranged from 0.01 to 10 mA (Model 225, Keithley Current Source, USA). Voltages were measured with a voltmeter (Model 197, Keithley, USA). The conductivity was calculated as

$$\sigma = \frac{1}{\rho} = \frac{1}{(V/I)wC(d/s)F(w/s)},$$

where σ is conductivity, ρ is resistivity, V is measured voltage, I is excitation current, w is width (pellet thickness), d is diameter, s is electrode spacing, and $C(d/s)$ and $F(w/s)$ are correction factors for sample geometry and finite thickness, respectively [16]. To ensure meaningful comparisons to other work, conductivities were normalized by the percent theoretical density of the sintered samples.

Optical measurements. The diffuse reflectance of as-fired pellets was measured from 190 to 850 nm using a double beam spectrophotometer with integrating sphere (Cary 1E with Cary 1/3 attachment, Varian, USA). A pressed PTFE (polytetrafluoroethylene) powder compact (Varian part number 04-101439-00) was used as a high transmission reference. A blackened sample mask was used to mount pellet samples. A background scan with the sample mask was performed and subtracted from all spectra. After diffuse reflectance, the samples were cut and the pellet cross-sections compared visually to the exterior surfaces. There were no visually discernible color differences.

Diffuse reflectance measurements on powders are roughly analogous to transmission measurements on thin films [17] Although absolute absorptions cannot be calculated from the diffuse reflectance spectra, bulk samples of different compositions can be compared to each other and the approximate optical band gap can be extracted. For samples with large ($\sim$ 5 microns or larger) grains, grain size effects on the spectra are minimal.

3. Phase relations

Overview. Table 1 lists the phases and lattice parameters observed in this study's samples. Fig. 1 shows the subsolidus $GaO_{1.5}$–SnO_2–ZnO phase diagram at 1250 °C as determined from consideration of the phases observed, lattice parameters and Gibbs' phase rule. No new structural compounds were discovered in the ternary system, but a new solid solubility was discovered between Zn_2SnO_4 and $ZnGa_2O_4$. The description of the phase relations is organized into discussion of

(a) the simple oxide end members,
(b) the three binary systems,
(c) the spinel join,
(d) the multi-phase regions in the diagram interior.

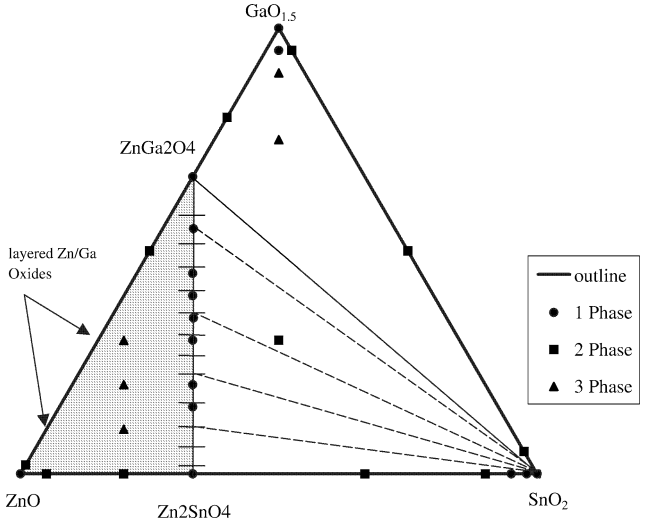

Fig. 1. Subsolidus phase diagram for the $GaO_{1.5}$–SnO_2–ZnO system at 1250 °C. Symbols show the number of phases detected by X-ray powder diffraction. Solid circles indicate single-phase compositions. Solid squares indicate two-phase compositions. Solid triangles indicate three-phase compositions. The shaded area indicates a region where phase relations were not determined.

3.1. Endpoints

Beta-Ga_2O_3 (referred to as $GaO_{1.5}$ here) has a monoclinic structure (C2/m) with half of the Ga^{3+} in tetrahedral coordination and half in octahedral coordination [18]. The lattice parameters of $GaO_{1.5}$ are $a = 12.23$ Å, $b = 3.04$ Å, $c = 5.80$ Å, and $\beta = 103.7°$ (JCPDS Card No. 43-1012). SnO_2 has the tetragonal, ($P4_2/mnm$) rutile structure with Sn^{4+} octahedrally coordinated [19]. The lattice parameters of SnO_2 are $a = 4.737$ Å and $c = 3.185$ Å (JCPDS Card No. 77-0452). ZnO has the hexagonal, ($P6_3mc$) wurtzite structure with Zn^{2+} tetrahedrally coordinated [20]. The lattice parameters of ZnO are $a = 3.2498$ Å and $c = 5.2066$ Å (JCPDS Card No. 80-0075).

3.2. Binary phase relations

3.2.1. $GaO_{1.5}$–SnO_2 binary

The $GaO_{1.5}$–SnO_2 binary consists entirely of a two-phase region between the two endpoints. Both the 5% SnO_2 and the 5% $GaO_{1.5}$ sample showed two-phase mixtures of the end member oxides by X-ray diffraction. The results of this study agree with previous work which showed minimal solubility of $GaO_{1.5}$ into SnO_2 or SnO_2 into $GaO_{1.5}$ [21]. The intermediate compound, Ga_4SnO_8, which has been reported to be stable at 1375 °C [21] and 1400 °C [22], was not seen.

3.2.2. ZnO–SnO_2 binary

The ZnO–SnO_2 binary contained one intermediate compound, Zn_2SnO_4, with two-phase regions between each end member and Zn_2SnO_4. The lattice parameters of Zn_2SnO_4 were unchanged (from the nominal value) in two-phase mixtures with ZnO or SnO_2, indicating minimal solubility of either oxide into the spinel. Also, both ZnO and SnO_2 had minimal solubility of the spinel.

A sample prepared with 95% ZnO showed the presence of Zn_2SnO_4. The lattice parameter of the ZnO in this sample was unchanged from pure ZnO, indicating minimal solid solubility. In addition, if Sn^{4+} was incorporated into ZnO, one would expect electrical conductivity in the sample. Electrical conductivity measurements showed no measurable conductivity ($\sigma < 0.01$ S cm^{-1}) in this sample.

In this study, spinel powder pattern peaks were noticeable in the 10% ZnO sample but were not visible in the 5% and 2% ZnO samples. Lattice parameter measurements of the SnO_2 in these samples showed very slight changes in lattice parameter with no correlation to Zn content. Previous work has shown small solubility ($\sim 0.7\%$) of ZnO into SnO_2 single crystals [23]. Paria and Maiti reported up to 20% solubility of ZnO into SnO_2, but did not characterize their samples [24]. We have displayed SnO_2 as a point compound.

3.2.3. $GaO_{1.5}$–ZnO binary

In the $GaO_{1.5}$–ZnO binary, we saw no noticeable solid solubilities, one well-characterized intermediate compound ($ZnGa_2O_4$), and complicated phase relations near ZnO. The lattice parameters of $ZnGa_2O_4$ and $GaO_{1.5}$ observed in a two-phase sample between the two compounds showed minimal difference from the nominal values, indicating minimal solid solubilities of the compounds. A two-phase, $ZnGa_2O_4$-containing sample on the ZnO side of $ZnGa_2O_4$ also showed an unchanged lattice parameter for the spinel, confirming that $ZnGa_2O_4$ is a line compound.

Wang et al. measured the solubility of $GaO_{1.5}$ in ZnO powders under reducing conditions (sealed tubes with Ga metal present) at 1200 and 1000 °C and noted a 2.7% solid solubility limit [25]. Nakamura et al. initially proposed a 20.5% solid solubility of $GaO_{1.5}$ into a distorted ZnO structure [26]. Subsequently they observed layered hexagonal compounds, $Zn_9Ga_2O_{12}$ and $Zn_{16}Ga_2O_{19}$, in sealed tube reactions at 1350 °C [27]. Nakamura et al. proposed that there is no high temperature equilibrium solid state solubility: $Zn_{1-x}Ga_xO_{1+0.5x}$, and that the equilibrium phase relations, instead, consist of homologous compounds $Zn_mGa_2O_{m+3}$ with m a large integer. Differences between the Wang and Nakamura reports may reflect an effect of oxygen on the solubility of Ga in ZnO. More reducing conditions may favor the solubility of Ga (doping), while more oxidizing conditions may favor formation of layered intergrowth structures.

In our samples between ZnO and $ZnGa_2O_4$, we noted several powder pattern peaks, which could not be assigned to either ZnO or $ZnGa_2O_4$. Even the 2% Ga-doped ZnO sample showed distortion of the ZnO peaks. The presence of layered intermediate compounds explains these results. Nakamura et al. noted extremely sluggish formation of the layered compounds at 1250 °C, which prompted them to prepare the compounds at higher temperatures in sealed tubes (to minimize ZnO volatility). With the techniques used in this

study (1250 °C heating in open containers), we were unable to definitively describe the phase relations in this area.

3.3. Zn_2SnO_4–$ZnGa_2O_4$ join

Zn_2SnO_4 (JCPDS Card No. 6-416) is a $+2/+4$, inverse spinel [28]. The unit cell is face-centered cubic (space group Fd-3m) with lattice parameter, $a = 8.6574$ Å. All Sn^{4+} are octahedrally coordinated. Zn^{2+} are distributed half in tetrahedral coordination, half in octahedral coordination. $ZnGa_2O_4$ (JCPDS Card No. 71-0843) is a normal spinel with an 8.330 lattice parameter. Anomalous dispersion X-ray diffraction has shown that Ga^{3+} is on the octahedral site and Zn^{2+} on the tetrahedral site [29].

Fig. 2 shows the lattice parameter as a function of composition on the Zn_2SnO_4–$ZnGa_2O_4$ join. Lattice parameter changes linearly (0.997 correlation coefficient) between the two end members, indicating a complete solid solution without changes in the normal cation site preferences. Zn_2SnO_4–$ZnGa_2O_4$ is similar to Zn_2SnO_4–$ZnFe_2O_4$, which shows a complete solid solution at 1060 °C [30]. However, lattice parameter versus composition deviates from linearity in the that system. Previously, we reported a similar partial solid solution achieved by substituting In^{3+} into Zn_2SnO_4: Zn_2SnO_4–$Zn_{1.55}In_{0.9}Sn_{0.55}O_4$ [31]. The incomplete solid solubility occurred because there was no $ZnIn_2O_4$ spinel end member [26,32–34].

3.4. Multi-phase regions

The interior of the phase diagram consists of three large multi-phase regions, all of which contain spinel as a component phase. $GaO_{1.5}$, SnO_2 and $ZnGa_2O_4$ form the endpoints of one three-phase triangle. Lattice parameter measurements of the phases of samples inside this triangle confirm the designation of $ZnGa_2O_4$ as the triangle endpoint and the designation of SnO_2 and $GaO_{1.5}$ as point compounds. There was minimal cosolubility of SnO_2 and ZnO into $GaO_{1.5}$. A sample prepared with 5% SnO_2, 5% ZnO, and 90% $GaO_{1.5}$ showed a three-phase powder pattern. A sample with 2.5% SnO_2, 2.5% ZnO, and 90% $GaO_{1.5}$ showed only β-gallia peaks. However, there was negligible change of the lattice parameters. This contrasts sharply with $InO_{1.5}$, where up to 40% of the cations could be replaced with SnO_2/ZnO co-substitution [35]. The reason for the low cosulubility extent is not clear. $GaO_{1.5}$ has octahedral sites and can accommodate large cations (for example up to 44% substitution by In^{3+}) [36].

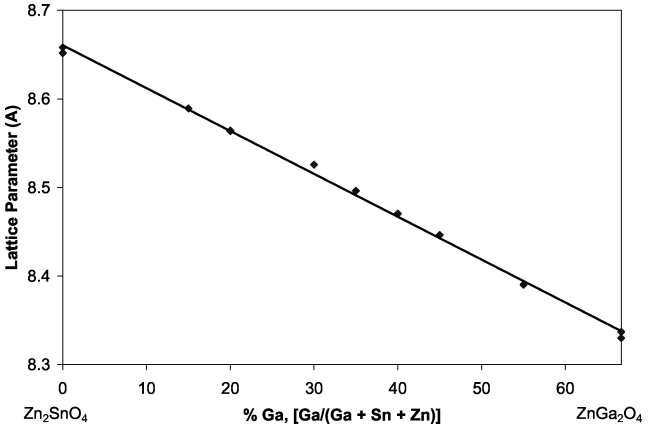

Fig. 2. Lattice parameter (Å) as a function of composition in the Zn_2SnO_4–$ZnGa_2O_4$ join.

SnO_2 and the spinel solid solution form the boundaries of a large two-phase region. The calculated (assuming SnO_2 as a point compound) and experimental tie lines for the sample in the two-phase region differed slightly. The calculated tie line predicted a spinel with 20% Ga^{3+}. The lattice parameter measurement showed a spinel with 23% Ga^{3+}. The calculated and observed lattice parameters agree fairly well given the methods used in the study. The small tie line discrepancy (3% Ga content) may result from incomplete reaction, ZnO evaporation, and/or lattice constant measurement error.

The phase region between ZnO and spinel is shown as a shaded region in Fig. 1 to indicate that the equilibrium phase relations are uncertain. Because of the slow kinetics of formation of the layered Zn/Ga oxides and the volatility of ZnO, we were unable to synthesize equilibrium samples in this region. All samples in the interior of this region contained spinel, ZnO, and other phase(s) believed to be layered Zn/Ga oxides.

4. Physical properties

Density and appearance. Theoretical densities were calculated from observed lattice parameters and starting mixture stoichiometry. Pellet densities were calculated directly from pellet mass and dimensions. Densities ranged from 50% to 65% of theoretical.

All the samples were bright white in color except those on the ZnO side of the spinel join, which were pale yellow. The 2% Ga-doped ZnO sample was white in color after its 1100 °C heating, but turned yellow during grinding under acetone. This pellet was visually white throughout the pellet cross-section and changed color slowly during grinding. ZnO is known to have different doping levels at grain boundaries and in grain interiors [37]. A possible explanation of the unusual color change is differences in Ga-doping levels in the grain interiors and grain boundaries.

Optical properties. Fig. 3 shows the diffuse reflectance (approximate transmission) spectra of unreduced and reduced spinel samples. In the visual wavelengths, all the samples showed better transparency than the high transmission reference (not shown) and would be expected to have better optical transmission than ITO.

The optical band gaps were estimated from the transmission onset wavelengths and are plotted in Fig. 5. Band

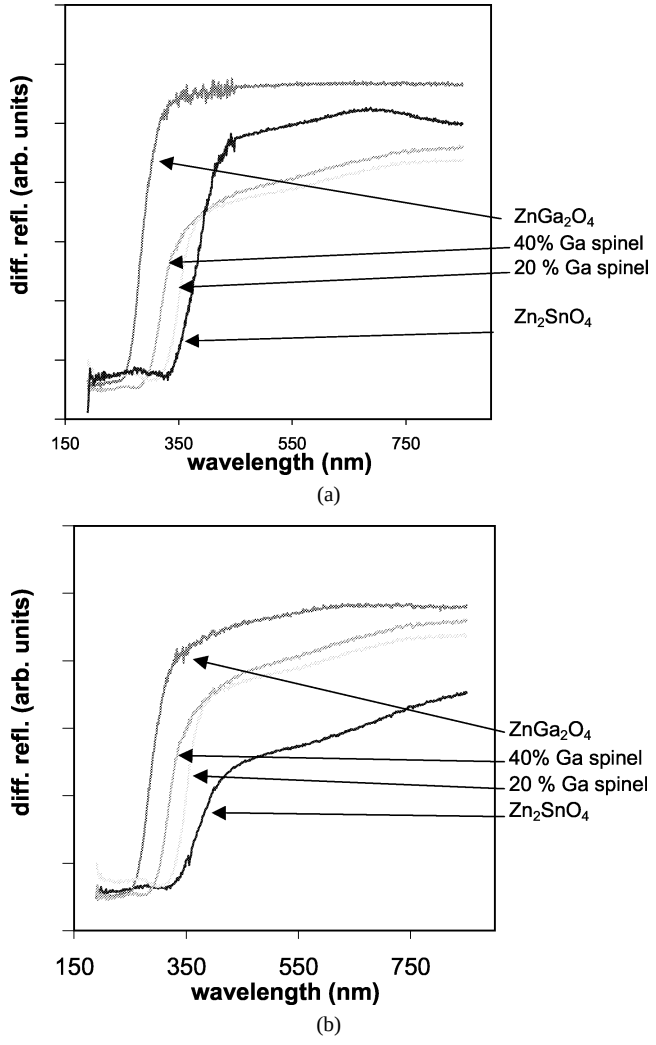

Fig. 3. Diffuse reflectance spectra of (a) as-fired spinel samples and (b) reduced spinel samples.

gap increased monotonically with increasing Ga composition from about 3.6 eV for Zn_2SnO_4 to about 4.7 eV for $ZnGa_2O_4$. Reduction slightly widened the band gap, with a more pronounced effect at lower gallium compositions. Previous work on In-substituted Zn_2SnO_4 showed a similar effect of reduction on band gap but an opposite effect of substitution on band gap [31].

Fig. 4 shows the before and after reduction diffuse reflectance spectra of 2% Ga-doped ZnO. The 3.2 eV band gap was unchanged by reduction.

Electrical properties. The spinel samples had negligible conductivity (< 0.01 S cm^{-1}) before and after reduction. Previous work on In-substituted Zn_2SnO_4 showed a differing trend. For that material, conductivity was measurable and increased with increasing In content.

The conductivity of the as-fired 2% Ga-doped ZnO pellet was 7 S cm^{-1}. After reduction, the conductivity was 125 S cm^{-1}. The conductivity of our reduced sample is comparable to that seen by Wang et al. in compressed

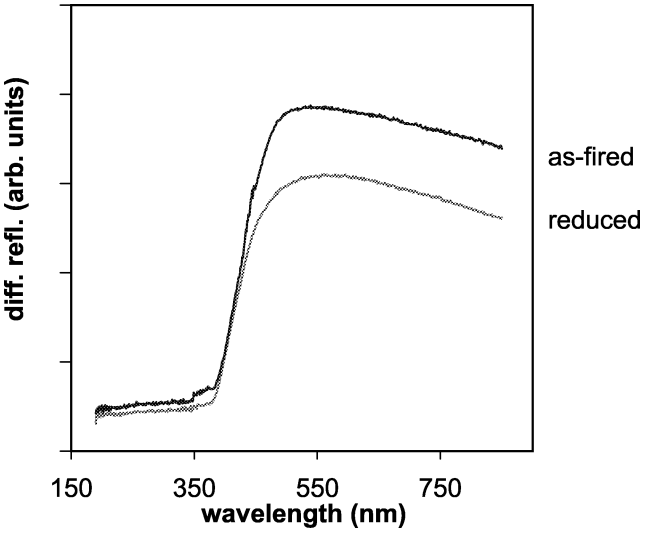

Fig. 4. Diffuse reflectance spectra of as-fired and reduced Ga-doped ZnO.

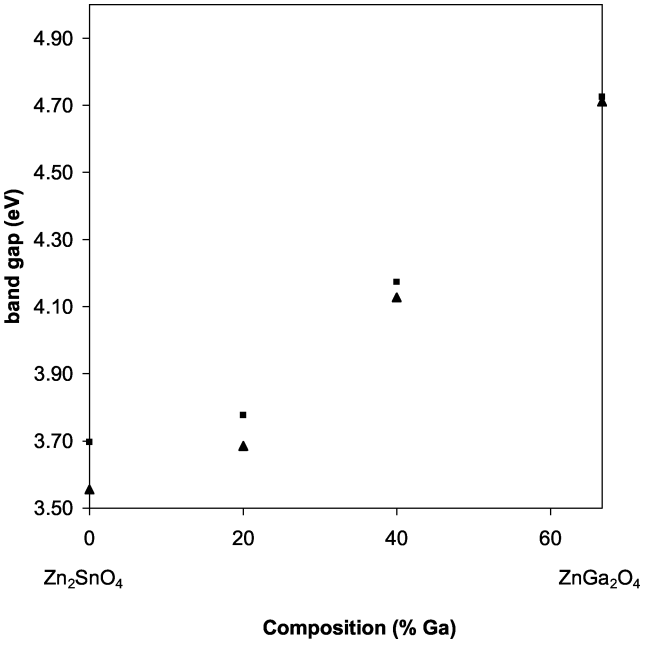

Fig. 5. Optical band gap versus composition for the as-fired (solid triangles) and reduced (solid squares) spinel samples.

powders of Ga-doped ZnO, but an order of magnitude less than that of Ga-doped ZnO films [25]. Multi-phase samples with compositions inside the shaded region in Fig. 1 had measurable conductivities that were less than the Ga-doped ZnO sample.

Application. Although bulk investigation, showed that the spinel solid solution has negligible conductivity and is thus a poor candidate for TCO applications, the spinel solid solution may be useful for other applications. Both end members of the solid solution have other optical (non-TCO) uses. $ZnGa_2O_4$ is a phosphor host material and is the subject of a great deal of research for this application [38]. Zn_2SnO_4

is a dielectric substrate in multi-component low-emissivity optical coatings [39]. The Zn_2SnO_4–$ZnGa_2O_4$ solid solution enables adjusting the lattice parameter and or the band gap of the end member spinels, while maintaining good optical transparency in the visual spectrum. This may prove useful in future non-TCO applications.

5. Conclusion

The Ga_2O_3–SnO_2–ZnO phase diagram was studied for relevancy to new TCO compositions. The diagram contained no new structural compounds but did contain a new solid solubility: the complete solution between Zn_2SnO_4 and $ZnGa_2O_4$. Although both end members have been reported as potential film TCOs, our bulk investigations showed negligible conductivity throughout the spinel solid solution. Optical band gap and lattice parameter varied monotonically with composition in Zn_2SnO_4–$ZnGa_2O_4$. The solid solution may have applicability to non-TCO optical uses of the spinel end members.

The only region of the ternary phase diagram with good conductivity was the phase region including Ga-doped ZnO. Phase relations near ZnO were not fully characterized because of the presence of slow-forming, layered Zn/Ga oxides. Further work is warranted to fully understand the structure–to property relations of the layered Zn/Ga oxides and their relationship to Ga-doped ZnO.

Acknowledgements

This work was supported by the MRSEC program of the National Science Foundation (DMR-0076097) at Northwestern University and made use of the Central Facilities of the same MRSEC program. George Palmer was supported by a National Defense Science and Engineering Graduate fellowship funded by the Office of Naval Research. Dr. Jon Schindler and Professor Carl Kannewurf of the Electrical and Computer Engineering Department at Northwestern University provided training on and use of the four probe conductivity apparatus.

References

[1] N.R. Lyman, in: Proceedings of the Symposium on Electrochromic Materials, Proc. Electrochem. Soc. 90-91 (1990) 201.
[2] I. Hamberg, C. Granqvist, J. Appl. Phys. 60 (1986) R123.
[3] D.D. Edwards, Phase relations, crystal structures, and electronic properties of select oxides in the Ga_2O_3–In_2O_3–SnO_2 system, Ph.D. Dissertation, Northwestern University, Evanston, IL, December, 1997.
[4] T. Moriga, D.R. Kammler, T.O. Mason, G.B. Palmer, K.R. Poeppelmeier, J. Am. Ceram. Soc. 81 (1999) 2705.
[5] G.B. Palmer, Phase relations and physical properties of transparent conductors in the (indium, gallium)–tin–zinc oxide systems, Ph.D. Dissertation, Northwestern University, Evanston, IL, December, 1999.
[6] G.B. Palmer, K.R. Poeppelmeier, D.D. Edwards, T.O. Mason, in: Proceedings of the Materials Research Society, Spring 1998, Symposium B: Flat Panel Display Materials and Large Area Processes, Proc. Mater. Res. Soc. 508 (1998) 308.
[7] Z.M. Jarzebski, J.P. Marton, J. Electrochem. Soc. 123 (1976) 199c, 299c, 333c.
[8] R. Wang, L.L.H. King, A.W. Sleight, J. Mater. Res. 11 (1996) 1659.
[9] J.M. Phillips, J. Kwo, G.A. Thomas, S.A. Carter, R.J. Cava, S.Y. Hou, J.J. Krajewski, J.H. Marshall, W.F. Peck, D.H. Rapkine, R.B. Vandover, Appl. Phys. Lett. 65 (1994) 115.
[10] T. Minami, S. Takata, T. Kakumu, J. Vac. Sci. Technol. A 14 (1996) 1989.
[11] D.D. Edwards, T.O. Mason, F. Goutenoire, K.R. Poeppelmeier, Appl. Phys. Lett. 70 (1997) 1706.
[12] X. Wu, T.J. Coutts, W.P. Mulligan, J. Vac. Sci. Technol. A 15 (1997) 1057.
[13] Z. Yan, H. Takei, H. Kawazoe, J. Am. Ceram. Soc. 81 (1998) 180.
[14] P. Georgopoulos, XRAYFIT Fortran program, Northwestern University, Evanston, IL, USA, 1993.
[15] D. Keszler, D. Cahen, J. Ibers, POLSQ Fortran program, Northwestern University, Evanston, IL, USA, 1984.
[16] F.M. Smits, Bell Syst. Tech. J. 37 (1958) 711.
[17] H. Hecht, in: W. Wendlandt (Ed.), Modern Aspects of Reflectance Spectroscopy, Plenum Press, New York, 1968, pp. 1–22.
[18] S. Geller, J. Chem. Phys. 33 (1960) 676.
[19] A. Roux, J. Cournot, C. R. Acad. Sci. 188 (1929) 1399.
[20] S.C. Abrahams, J.L. Bernstein, Acta Crystallogr., Sect. B 25 (1969) 1233.
[21] D.D. Edwards, T.O. Mason, J. Am. Ceram. Soc. 81 (1998) 3285.
[22] M.B. Varfolomeev, A.S. Miranova, T.I. Dudina, Koldashov, Russ. J. Inorg. Chem. 20 (1975) 1738.
[23] K.W. Balts, Conductivity changes due to chemisorption on zinc-doped polycrystalline stannic oxide, M.S. Thesis, Oklahoma State University, 1970.
[24] M.K. Paria, H.S. Maiti, J. Mater. Sci. 18 (1983) 2101.
[25] R. Wang, A.W. Sleight, Chem. Mater. 8 (1996) 433.
[26] M. Nakamura, N. Kimizuka, T. Mohri, J. Solid State Chem. 93 (1991) 298.
[27] N. Kimizuka, M. Isobe, M. Nakamura, J. Solid State Chem. 116 (1995) 170.
[28] T. Barth, E. Posnjak, Z. Kristallogr. 82 (1932) 325.
[29] J. Goffin, Baffier, Noel, M. Huber, C. R. Acad. Sci. 252 (1961) 2744.
[30] R. Tyson, L. Chang, J. Am. Ceram. Soc. 64 (1981) C-4.
[31] G.B. Palmer, K.R. Poeppelmeier, T.O. Mason, J. Solid State Chem. 134 (1997) 192.
[32] V.H. Kasper, Z. Anorg. Allg. Chem. 349 (1967) 113.
[33] P.J. Cannard, R.J.D. Tilley, J. Solid State Chem. 73 (1988) 418.
[34] T. Moriga, D.D. Edwards, T.O. Mason, G.B. Palmer, K.R. Poeppelmeier, J.L. Schindler, C.R. Kannewurf, I. Nakabayashi, J. Am. Ceram. Soc. 81 (1998) 1310.
[35] G.B. Palmer, K.R. Poeppelmeier, T.O. Mason, Chem. Mater. 9 (1997) 3121.
[36] D.D. Edwards, P.E. Folkins, T.O. Mason, J. Am. Ceram. Soc. 80 (1997) 253.
[37] A.B. Glot, in: L.M. Levisnon (Ed.), Advances in Varistor Technology: Ceramic Transactions, Vol. 3, 1989, pp. 194–203.
[38] W.S. Hong, L.C. De Jonghe, J. Am. Ceram. Soc. 78 (1995) 3217.
[39] M. Arbab, MRS Bull. 22 (9) (1997) 27.